Interpretation of $Z_b(10610)$ and $Z_b(10650)$ in the ISPE mechanism and the Charmonium Counterpart [*]

CHEN Dian-Yong(陈殿勇)[1,3;1)]   LIU Xiang(刘翔)[2,3;2)]   Takayuki Matsuki[4;3)]

[1] Nuclear Theory Group, Institute of Modern Physics of Chinese Academy of Sciences, Lanzhou 730000, China
[2] School of Physical Science and Technology, Lanzhou University, Lanzhou 730000, China
[3] Research Center for Hadron and CSR Physics, Lanzhou University and Institute of Modern Physics of Chinese Academy of Sciences, Lanzhou 730000, China
[4] Tokyo Kasei University, 1-18-1 Kaga, Itabashi, Tokyo 173-8602, Japan

Abstract: The initial single pion emission (ISPE) mechanism is applied to the processes $\Upsilon(5S) \to \pi B^{(*)}\bar{B}^{(*)}$, whose details have been recently reported at ICHEP2012, and we obtain reasonable agreement with Bell's measurements; that is, we succeed in reproducing the enhancement structures of $Z_b(10610)$ and $Z_b(10650)$. Inspired by this success, we also predict the corresponding enhancement structures in open charm one-pion decays of higher charmonia near the thresholds of $D^*\bar{D}$ and $D^*\bar{D}^*$.

Key words: $Z_b(10610)$, $Z_b(10650)$, ISPE mechanism, Charmonium Counterpart

PACS: 13.25.Gv, 14.40.Pq, 13.75.Lb   **DOI:** 10.1088/1674-1137/38/5/053102

1   Introduction

Two charged bottomonium-like structures, $Z_b(10610)$ and $Z_b(10650)$, were reported by the Belle Collaboration in the hidden-bottom decays of $\Upsilon(5S)$ [1]. As indicated by the analysis of the corresponding $\pi^{\pm}\Upsilon(nS)$ (n=1,2,3) and $\pi^{\pm}h_b(mP)$ (m=1,2) invariant mass spectra, $Z_b(10610)$ and $Z_b(10650)$ are two narrow structures with masses and widths $M_{Z_b(10610)}$=(10607.2±2.0) MeV, $\Gamma_{Z_b(10610)} = (18.4\pm2.4)$ MeV, $M_{Z_b(10650)} = (10652.2\pm1.5)$ MeV, and $\Gamma_{Z_b(10650)}$=(11.5±2.2) MeV, respectively [1]. In addition, the spin-parity quantum numbers are $J^P = 1^+$ for both $Z_b(10610)$ and $Z_b(10650)$ due to the analysis of charged pion angular distributions [2].

Observation of these two structures has inspired the interest of many theorists. Various theoretical explanations were proposed after the Belle's observation. In the following paper, we will briefly review the research status on $Z_b(10610)$ and $Z_b(10650)$.

Considering that $Z_b(10610)$ and $Z_b(10650)$ are charged and close to $B\bar{B}^*$ and $B^*\bar{B}^*$ thresholds, respectively, many theoretical efforts have been made to answer the question of whether these newly observed structures are real exotic states or not. Before the discovery of $Z_b(10610)$ and $Z_b(10650)$, the authors in Refs. [3, 4] predicted the existence of loosely bound S-wave $B\bar{B}^*$ molecular states. The heavy quark spin structure that was developed by Bondar et al. [5], the chiral constituent quark model approach in Ref. [6], the effective Lagrangian approach via the one-boson exchange in Ref. [7], and the study of the line shape in the vicinity of $B^{(*)}\bar{B}^{(*)}$ thresholds, as well as two-body decay rates using effective field theory in Ref. [8], have all shown that $Z_b(10610)$ and $Z_b(10650)$ can be the $B\bar{B}^*$ and $B^*\bar{B}^*$ molecular states, respectively. The authors in Ref. [6] further showed that their quantum numbers are $I(J^P) = 1(1^+)$. The QCD sum rule (QSR) analysis that was developed by Zhang et al. [9] suggested that $Z_b(10610)$ could be a $B\bar{B}^*$ molecular state. Using the Bethe-Salpeter equation, the problem of whether $Z_b(10610)$ is a $B\bar{B}^*$ molecular state was studied in Ref. [10], which claimed that $B\bar{B}^*$ molecular state with isospin $I=1$ cannot be formed when the contribution of the σ exchange is small [10].

Apart from these studies on mass spectrum, there are

also some theoretical papers that have been dedicated to the production and decay behavior of $Z_b(10610)$ and $Z_b(10650)$. Under the frameworks of $B\bar{B}^*$ and $B^*\bar{B}^*$ molecular states, the radiative decay of $\Upsilon(5S)$ into molecular bottomonium was calculated [11], and the processes of $Z_b(10610)$ and $Z_b(10650)$ decaying into bottomonium and pion were also recently investigated [12]. In Ref. [13], the properties of $Z_b(10610)$ and $Z_b(10650)$ were studied, assuming that they are $B\bar{B}^*$ and $B^*\bar{B}^*$ molecular states. Dong et al. [14] performed the calculation of molecular hadrons, $Z_b(10610)$ and $Z_b(10650)$, decaying into $\Upsilon(nS)$ and π^+ by the effective Lagrangian approach.

A tetraquark explanation for $Z_b(10610)$ and $Z_b(10650)$ has also been proposed. In Ref. [15], the masses of tetraquark states $bu\bar{b}\bar{d}$ and $bd\bar{b}\bar{u}$ with $J^P=1^+$ were obtained by the chromomagnetic interaction Hamiltonian, and they are compatible with the corresponding masses of $Z_b(10610)$ and $Z_b(10650)$. Using the QSR approach, the authors in Ref. [16] calculated the mass of the tetraquark states with the configuration $[bd][\bar{b}\bar{u}]$ and found that $Z_b(10610)$ and $Z_b(10650)$ can be described by tetraquark. Ali et al. also gave a tetraquark interpretation for $Z_b(10610)$ and $Z_b(10650)$ and studied the decay of a tetraquark state $Y_b(10890)$ into $Z_b(10610)^{\pm}\pi^{\mp}$ or $Z_b(10650)^{\pm}\pi^{\mp}$, and the decays of $Z_b(10610)/Z_b(10650)$ into $\pi^{\pm}\Upsilon(nS)$ and $\pi^{\pm}h_b(mP)$ [17].

Besides proposing exotic states to understand these structures, theorists have also tried to explain why $Z_b(10610)$ and $Z_b(10650)$ were observed in the hidden-bottom decays of $\Upsilon(5S)$. Bugg suggested that the two observed structures of $Z_b(10610)$ and $Z_b(10650)$ are due to cusp effects [18]. The authors in Ref. [19] indicated that newly observed $Z_b(10610)$ and $Z_b(10650)$ play an important role in describing Belle's previous observation of the anomalous $\Upsilon(2S)\pi^+\pi^-$ production near the peak of $\Upsilon(5S)$ at $\sqrt{s}=10.87$ GeV [20], where the resulting distributions, $d\Gamma(\Upsilon(5S)\to\Upsilon(2S)\pi^+\pi^-)/dm_{\pi^+\pi^-}$ and $d\Gamma(\Upsilon(5S)\to\Upsilon(2S)\pi^+\pi^-)/d\cos\theta$, agree with Belle's measurements after inclusion of these Z_b states [19]. Later, the initial single pion emission (ISPE) mechanism was proposed in the $\Upsilon(5S)$ hidden-bottom dipion decays, where the line shapes of $d\Gamma(\Upsilon(5S)\to\Upsilon(nS)\pi^+\pi^-))/dm_{\Upsilon(nS)\pi^+}$ $(n=1,2,3)$ and $d\Gamma(\Upsilon(5S)\to h_b(mP)\pi^+\pi^-))/dm_{h_b(mP)\pi^+}$ $(m=1,2)$ are given [21]. The sharp structures obtained around 10610 MeV and 10650 MeV in the theoretical line shapes of these distributions could naturally correspond to the $Z_b(10610)$ and $Z_b(10650)$ structures that were newly observed by Belle [21].

Although there have been many theoretical efforts to clarify $Z_b(10610)$ and $Z_b(10650)$, further study of these two Z_b states is still an interesting research topic. For instance, it is crucial to distinguish between different explanations for $Z_b(10610)$ and $Z_b(10650)$. Very recently, the Belle Collaboration has reported new results on $Z_b(10610)$ and $Z_b(10650)$ at the ICHEP2012 conference, and have found that these Z_b structures also exist in the $B\bar{B}^*$ and $B^*\bar{B}^*$ invariant mass spectra of $\Upsilon(5S)\to\pi B\bar{B}^*$, $\pi B^*\bar{B}^*$ decays [22]. This new experimental phenomenon of $Z_b(10610)$ and $Z_b(10650)$ can provide an important platform to test the explanations for $Z_b(10610)$ and $Z_b(10650)$ that have been proposed so far. This process also motivates us to apply the ISPE mechanism.

In this work, we will explain why two charged structures $Z_b(10610)$ and $Z_b(10650)$ can appear in the $B\bar{B}^*$ and $B^*\bar{B}^*$ invariant mass spectra of the $\Upsilon(5S)\to\pi B\bar{B}^*$, $\pi B^*\bar{B}^*$ decays. We find that the ISPE mechanism proposed in Ref. [21] can be well applied to the $\Upsilon(5S)\to \pi B\bar{B}^*$, $\pi B^*\bar{B}^*$ processes, which can further test this mechanism. Other than explaining the Belle's new observation, we will extend our study of the open-charm decays of higher charmonia with the emission of a single pion because of the similarity between bottomonium and charmonium [23]. As a result of our study, we will give the corresponding prediction of two charged charmonium-like structures close to the $D^*\bar{D}$ and $D^*\bar{D}^*$ thresholds, which can be found in the invariant mass spectra $m_{D^*\bar{D}}$ and $m_{D^*\bar{D}^*}$ of the open-charm decays of higher charmonia with the emission of a single pion.

This work is organized as follows. After a brief explanation, we introduce the ISPE mechanism and its application to $\Upsilon(5S)\to\pi B\bar{B}^*$. The next section will examine $\pi B^*\bar{B}^*$ decays. In addition, the relevant numerical results will be presented. In Section 3, we extend the ISPE mechanism to study the open-charm decays of higher charmonia with the emission of a single pion and give the corresponding predictions. This paper ends with summary in Section 4.

2   The ISPE mechanism and the $\Upsilon(5S)\to\pi B^{(*)}\bar{B}^{(*)}$ decays

The ISPE mechanism was first proposed to study the $\Upsilon(5S)\to\Upsilon(nS)\pi^+\pi^-$ $(n=1,2,3)$ and $\Upsilon(5S)\to h_b(mP)\pi^+\pi^-$ $(m=1,2)$ decays [21]. It also explains why two Z_b structures can be observed in these processes. Via the ISPE mechanism, the hidden-bottom dipion decays of $\Upsilon(5S)$ can occur through two steps. First, $\Upsilon(5S)$ decays into the $B^{(*)}\bar{B}^{(*)}$ plus one pion, where the emitted pion has continuous energy distribution. Secondly, the $B^{(*)}$ and $\bar{B}^{(*)}$ mesons with low momentum can easily interact with each other to convert into the final state $\Upsilon(nS)\pi$ or $h_b(mP)\pi$ via the $B^{(*)}$ meson exchange [21].

In this paper, we would like to apply the ISPE mechanism to the open-bottom decays of $\Upsilon(5S)$ with the emission of a single pion. In Figs. 1 and 2, we present the typical diagrams describing $\Upsilon(5S)\to\pi B^{(*)}\bar{B}^{(*)}$ via the
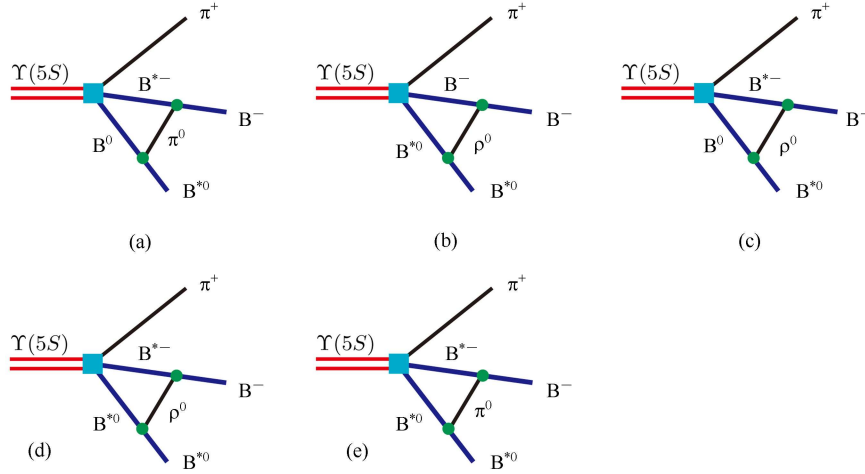
Fig. 1.   (color online.) The typical diagrams for the $\Upsilon(5S)\to B^{*0}B^-\pi^+$ decays via the ISPE mechanism. One can obtain the other diagrams by replacing π^0 and ρ^0 with η and ω, respectively.

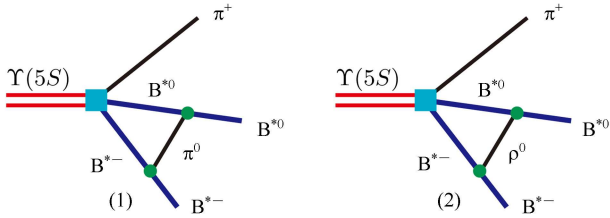Fig. 2.   (color online.) The schematic diagrams for the $\Upsilon(5S)\to B^{*0}B^{*-}\pi^+$ decays by the ISPE mechanism. Replacing the exchanged π^0 by η and ρ^0 by ω, one can generate the other diagrams.

ISPE mechanism, where the intermediate $B^{(*)}$ and $\bar{B}^{(*)}$ meson can be converted into $B\bar{B}^*$ or $B^*\bar{B}^*$ final state by exchanging light mesons, such as π, η, ρ and ω.

In the following paper, we will write out the decay amplitudes corresponding to the diagrams listed in Figs. 1 and 2. The effective Lagrangians that are relevant to our study are given by

$$
\begin{aligned}
\mathcal{L}_{\Upsilon(5S)\mathcal{B}^{(*)}\bar{\mathcal{B}}^{(*)}\pi} = {} & -ig_{\Upsilon'\mathcal{B}\mathcal{B}\pi}\varepsilon^{\mu\nu\alpha\beta}\Upsilon_\mu\partial_\nu\mathcal{B}\partial_\alpha\pi\partial_\beta\bar{\mathcal{B}} \\
& +g_{\Upsilon\mathcal{B}^*\mathcal{B}\pi}\Upsilon^\mu(\mathcal{B}\pi\bar{\mathcal{B}}^*_\mu+\mathcal{B}^*_\mu\pi\bar{\mathcal{B}}) \\
& -ig_{\Upsilon\mathcal{B}^*\mathcal{B}^*\pi}\varepsilon^{\mu\nu\alpha\beta}\Upsilon_\mu\mathcal{B}^*_\nu\partial_\alpha\pi\bar{\mathcal{B}}^*_\beta \\
& -ih_{\Upsilon\mathcal{B}^*\mathcal{B}^*\pi}\varepsilon^{\mu\nu\alpha\beta}\partial_\mu\Upsilon_\nu\mathcal{B}^*_\alpha\pi\bar{\mathcal{B}}^*_\beta, \quad (1)
\end{aligned}
$$

$$
\begin{aligned}
\mathcal{L}_{\mathcal{B}^{(*)}\mathcal{B}^{(*)}\mathcal{V}} = {} & -ig_{\mathcal{B}\mathcal{B}\mathcal{V}}\bar{\mathcal{B}}\overleftrightarrow{\partial}_\mu\mathcal{B}(\mathcal{V}^\mu)-2f_{\mathcal{B}\mathcal{B}^*\mathcal{V}}\epsilon_{\mu\nu\alpha\beta} \\
& \times(\partial^\mu\mathcal{V}^\nu)(\bar{\mathcal{B}}\overleftrightarrow{\partial}^\alpha\mathcal{B}^{*\beta}-\bar{\mathcal{B}}^{*\beta}\overleftrightarrow{\partial}^\alpha\mathcal{B}) \\
& +ig_{\mathcal{B}^*\mathcal{B}^*\mathcal{V}}\bar{\mathcal{B}}^{*\nu}\overleftrightarrow{\partial}_\mu\mathcal{B}^*_\nu(\mathcal{V}^\mu) \\
& +4if_{\mathcal{B}^*\mathcal{B}^*\mathcal{V}}\bar{\mathcal{B}}^{*\mu}(\partial_\mu\mathcal{V}_\nu-\partial_\nu\mathcal{V}_\mu)\mathcal{B}^{*\nu}, \quad (2)
\end{aligned}
$$

$$
\begin{aligned}
\mathcal{L}_{\mathcal{B}^*\mathcal{B}^{(*)}\mathcal{P}} = {} & -ig_{\mathcal{B}^*\mathcal{B}\mathcal{V}}(\bar{\mathcal{B}}_i\partial_\mu\mathcal{P}_{ij}\mathcal{B}^{*\mu}_j-\bar{\mathcal{B}}^{*\mu}_i\partial_\mu\mathcal{P}_{ij}\mathcal{B}_j) \\
& +\frac{1}{2}g_{\mathcal{B}^*\mathcal{B}^*\mathcal{P}}\epsilon_{\mu\nu\alpha\beta}\bar{\mathcal{B}}^{*\mu}_i\partial^\nu\mathcal{P}_{ij}\overleftrightarrow{\partial}^\alpha\mathcal{B}^{*\beta}_j, \quad (3)
\end{aligned}
$$

where $\mathcal{V}$ and $\mathcal{P}$ are 3×3 matrices corresponding to the pseudoscalar and vector octets, which satisfy

$$
\mathcal{V} = \begin{pmatrix} \dfrac{\rho^0}{\sqrt{2}}+\dfrac{\omega}{\sqrt{2}} & \rho^+ & K^{*+} \\[2mm] \rho^- & -\dfrac{\rho^0}{\sqrt{2}}+\dfrac{\omega}{\sqrt{2}} & K^{*0} \\[2mm] K^{*-} & \bar{K}^{*0} & \phi \end{pmatrix},
$$

$$
\mathcal{P} = \begin{pmatrix} \dfrac{\pi^0}{\sqrt{2}}+\alpha\eta+\beta\eta' & \pi^+ & K^+ \\[2mm] \pi^- & -\dfrac{\pi^0}{\sqrt{2}}+\alpha\eta+\beta\eta' & K^0 \\[2mm] K^- & \bar{K}^0 & \gamma\eta+\delta\eta' \end{pmatrix}, \quad (4)
$$

the parameters α, β, γ and δ can be related to the mixing angle θ by

$$
\alpha=\frac{\cos\theta-\sqrt{2}\sin\theta}{\sqrt{6}}, \quad \beta=\frac{\sin\theta+\sqrt{2}\cos\theta}{\sqrt{6}},
$$

$$
\gamma=\frac{-2\cos\theta-\sqrt{2}\sin\theta}{\sqrt{6}}, \quad \delta=\frac{-2\sin\theta+\sqrt{2}\cos\theta}{\sqrt{6}}. \quad (5)
$$

In the present work we adopt $\theta=-19.1^\circ$ [24, 25], which is determined from J/ψ decay. These effective Lagrangians are constructed by considering heavy quark limit and chiral symmetry. The coupling constants in the above Lagrangians can be defined as $g_{B^*B^*\pi}=g_{B^*B\pi}/\sqrt{m_B m_{B^*}}=2g/f_\pi$ and $g_{BB\omega}=g_{B^*B^*\omega}=\beta g_V/\sqrt{2}$, $f_{B^*B^*\rho}/m_{B^*}=f_{BB^*\rho}=\lambda m_\rho/(\sqrt{2}f_\pi)$, where $g_V=m_\rho/f_\pi$, $\beta=0.9$, $\lambda=0.56$ GeV^{-1} and $f_\pi=132$ MeV.

Using the above Lagrangians, we obtain the decay amplitudes for $\Upsilon(5S)\to B^{*0}B^-\pi^+$, corresponding to the five diagrams shown in Fig. 1 as

$$\mathcal{M}_{\mathrm{a}} = (\mathrm{i})^3 \int \frac{\mathrm{d}^4 q}{(2\pi)^4} [g_{\Upsilon\mathrm{B}^*\mathrm{B}\pi}\epsilon_\Upsilon^\mu][-\mathrm{i}g_{\mathrm{B}^*\mathrm{B}\pi}(\mathrm{i}q_\rho)][-\mathrm{i}g_{\mathrm{B}^*\mathrm{B}\pi}(-\mathrm{i}q^\nu)\epsilon_{\mathrm{B}^*}^\nu]\frac{-g^{\mu\rho}+p_1^\mu p_1^\rho/m_{\mathrm{B}^*}^2}{p_1^2-m_{\mathrm{B}^*}^2}\frac{1}{p_2^2-m_{\mathrm{B}}^2}\frac{1}{q^2-m_{\mathrm{B}}^2}\mathcal{F}^2(q^2,m_\pi^2),$$

$$\mathcal{M}_{\mathrm{b}} = (\mathrm{i})^3 \int \frac{\mathrm{d}^4 q}{(2\pi)^4} [g_{\Upsilon\mathrm{B}^*\mathrm{B}\pi}\epsilon_\Upsilon^\mu][-\mathrm{i}g_{\mathrm{BB}\rho}(-\mathrm{i}p_{1\rho}+\mathrm{i}p_{4\rho})][\mathrm{i}g_{\mathrm{B}^*\mathrm{B}^*\rho}(\mathrm{i}p_{5\beta}-\mathrm{i}p_{2\beta})\epsilon_{\mathrm{B}^*}^\nu g_{\alpha\nu}+4\mathrm{i}f_{\mathrm{B}^*\mathrm{B}^*\rho}(-\mathrm{i}q_\alpha g_{\nu\beta}$$

$$+\mathrm{i}q_\beta g_{\nu\alpha})\epsilon_{\mathrm{B}^*}^\nu]\frac{1}{p_1^2-m_{\mathrm{B}}^2}\frac{-g^{\mu\alpha}+p_2^\mu p_2^\alpha/m_{\mathrm{B}^*}^2}{p_2^2-m_{\mathrm{B}^*}^2}\frac{-g^{\rho\beta}+q^\rho q^\beta/m_\rho^2}{q^2-m_\rho^2}\mathcal{F}^2(q^2,m_\rho^2),$$

$$\mathcal{M}_{\mathrm{c}} = (\mathrm{i})^3 \int \frac{\mathrm{d}^4 q}{(2\pi)^4} [g_{\Upsilon\mathrm{B}^*\mathrm{B}\pi}\epsilon_\Upsilon^\mu][-2f_{\mathrm{B}^*\mathrm{B}\rho}\varepsilon_{\rho\lambda\alpha\beta}(\mathrm{i}q^\rho)(-\mathrm{i}p_1^\alpha-\mathrm{i}p_4^\alpha)][-2f_{\mathrm{B}^*\mathrm{B}\rho}\varepsilon_{\theta\phi\delta\nu}(-\mathrm{i}q^\theta)(\mathrm{i}p_5^\delta+\mathrm{i}p_2^\delta)\epsilon_{\mathrm{B}^*}^\nu]$$

$$\times\frac{-g^{\mu\beta}+p_1^\mu p_1^\beta/m_{\mathrm{B}^*}^2}{p_1^2-m_{\mathrm{B}^*}^2}\frac{1}{p_2^2-m_{\mathrm{B}}^2}\frac{-g^{\lambda\phi}+q^\lambda q^\phi/m_{\mathrm{B}^*}^2}{q^2-m_{\mathrm{B}^*}^2}\mathcal{F}^2(q^2,m_\rho^2),$$

$$\mathcal{M}_{\mathrm{d}} = (\mathrm{i})^3 \int \frac{\mathrm{d}^4 q}{(2\pi)^4} [-\mathrm{i}g_{\Upsilon\mathrm{B}^*\mathrm{B}^*\pi}\varepsilon_{\mu\nu\alpha\beta}\epsilon_\Upsilon^\mu(\mathrm{i}p_3^\alpha)-\mathrm{i}h_{\Upsilon\mathrm{B}^*\mathrm{B}^*\pi}\varepsilon_{\alpha\mu\nu\alpha}(-\mathrm{i}p_0^\alpha)\epsilon_\Upsilon^\mu][-2f_{\mathrm{B}^{*-}\mathrm{B}^-\rho^0}\varepsilon_{\delta\tau\theta\phi}(\mathrm{i}q^\delta)(-\mathrm{i}p_1^\theta-\mathrm{i}p_4^\theta)]$$

$$\times[\mathrm{i}g_{\mathrm{B}^{*0}\mathrm{B}^{*0}\rho^0}((\mathrm{i}p_{5\rho}+\mathrm{i}p_{2\rho})g_{\lambda\omega}\epsilon_{\mathrm{B}^*}^\omega)+4\mathrm{i}f_{\mathrm{B}^{*0}\mathrm{B}^{*0}\rho^0}(-\mathrm{i}q_\lambda g_{\rho\omega}+\mathrm{i}q_\omega g_{\lambda\rho})\epsilon_{\mathrm{B}^*}^\omega]$$

$$\times\frac{-g^{\beta\phi}+p_1^\beta p_1^\phi/m_{\mathrm{B}^*}^2}{p_1^2-m_{\mathrm{B}^*}^2}\frac{-g^{\nu\lambda}+p_2^\nu p_2^\lambda/m_{\mathrm{B}^*}^2}{p_2^2-m_{\mathrm{B}^*}^2}\frac{-g^{\tau\rho}+q^\tau q^\rho/m_\rho^2}{q^2-m_\rho^2}\mathcal{F}^2(q^2,m_\rho^2),$$

$$\mathcal{M}_{\mathrm{e}} = (\mathrm{i})^3 \int \frac{\mathrm{d}^4 q}{(2\pi)^4} [-\mathrm{i}g_{\Upsilon\mathrm{B}^*\mathrm{B}^*\pi}\varepsilon_{\mu\nu\alpha\beta}\epsilon_\Upsilon^\mu(\mathrm{i}p_3^\alpha)-\mathrm{i}h_{\Upsilon\mathrm{B}^*\mathrm{B}^*\pi}\varepsilon_{\alpha\mu\nu\alpha}(-\mathrm{i}p_0^\alpha)\epsilon_\Upsilon^\mu][\mathrm{i}g_{\mathrm{B}^{*-}\mathrm{B}^-\pi^0}(-\mathrm{i}q^\rho)]$$

$$\times[-g_{\mathrm{B}^{*0}\mathrm{B}^{*0}\pi^0}\varepsilon_{\delta\omega\theta\phi}(\mathrm{i}p_5^\delta)\epsilon_{\mathrm{B}^*}^\omega(-\mathrm{i}p_2^\theta)]\frac{-g^{\beta\rho}+p_1^\beta p_1^\rho/m_{\mathrm{B}^*}^2}{p_1^2-m_{\mathrm{B}^*}^2}\frac{-g^{\nu\phi}+p_2^\nu p_2^\phi/m_{\mathrm{B}^*}^2}{p_2^2-m_{\mathrm{B}^*}^2}\frac{1}{q^2-m_\pi^2}\mathcal{F}^2(q^2,m_\pi^2). \tag{6}$$

Similarly, one also gets the amplitudes corresponding to the two diagrams listed in Fig. 2 as

$$\mathcal{M}_1 = (\mathrm{i})^3 \int \frac{\mathrm{d}^4 q}{(2\pi)^4} [-\mathrm{i}g_{\Upsilon\mathrm{B}^*\mathrm{B}^*\pi}\varepsilon_{\mu\lambda\alpha\beta}\epsilon_\Upsilon^\mu(\mathrm{i}p_3^\alpha-\mathrm{i}p_0^\alpha)][-g_{\mathrm{B}^*\mathrm{B}^*\pi}\varepsilon_{\delta\tau\theta\nu}(-\mathrm{i}p_1^\delta)(\mathrm{i}p_4^\theta)\epsilon_{\mathrm{B}^*}^\nu][-g_{\mathrm{B}^*\mathrm{B}^*\pi}\varepsilon_{\phi\rho\zeta\kappa}(\mathrm{i}p_5^\phi)\epsilon_{\mathrm{B}^*}^\rho(-\mathrm{i}p_2^\zeta)]$$

$$\times\frac{-g^{\lambda\tau}+p_1^\lambda p_1^\tau/m_{\mathrm{B}^*}^2}{p_1^2-m_{\mathrm{B}^*}^2}\frac{-g^{\beta\kappa}+p_2^\beta p_2^\kappa/m_{\mathrm{B}^*}^2}{p_2^2-m_{\mathrm{B}^*}^2}\frac{1}{q^2-m_\pi^2}\mathcal{F}^2(q^2,m_\pi^2),$$

$$\mathcal{M}_2 = (\mathrm{i})^3 \int \frac{\mathrm{d}^4 q}{(2\pi)^4} [-\mathrm{i}g_{\Upsilon\mathrm{B}^*\mathrm{B}^*\pi}\varepsilon_{\mu\lambda\alpha\beta}\epsilon_\Upsilon^\mu(\mathrm{i}p_3^\alpha-\mathrm{i}p_0^\alpha)][\mathrm{i}g_{\mathrm{B}^*\mathrm{B}^*\rho}(\mathrm{i}p_{4\delta}+\mathrm{i}p_{1\delta})\epsilon_{\mathrm{B}^*}^\nu g_{\nu\theta}+4\mathrm{i}f_{\mathrm{B}^*\mathrm{B}^*\rho}(\mathrm{i}q_\theta g_{\nu\delta}-\mathrm{i}q_\nu g_{\theta\delta})\epsilon_{\mathrm{B}^*}^\nu]$$

$$\times[\mathrm{i}g_{\mathrm{B}^*\mathrm{B}^*\rho}(-\mathrm{i}p_{2\tau}-\mathrm{i}p_{5\tau})\epsilon_{\mathrm{B}^*}^\rho g_{\rho\zeta}+4\mathrm{i}f_{\mathrm{B}^*\mathrm{B}^*\rho}(-\mathrm{i}q_\zeta g_{\rho\tau}+\mathrm{i}q_\rho g_{\zeta\tau})\epsilon_{\mathrm{B}^*}^\rho]\frac{-g^{\lambda\theta}+p_1^\lambda p_1^\theta/m_{\mathrm{B}^*}^2}{p_1^2-m_{\mathrm{B}^*}^2}$$

$$\times\frac{-g^{\beta\zeta}+p_2^\beta p_2^\zeta/m_{\mathrm{B}^*}^2}{p_2^2-m_{\mathrm{B}^*}^2}\frac{-g^{\delta\tau}+q^\delta q^\tau/m_\rho^2}{q^2-m_\rho^2}\mathcal{F}^2(q^2,m_\rho^2).$$

In these expressions for decay amplitudes, the dipole form factor (FF)

$$\mathcal{F}(q^2,m^2)=\left(\frac{\Lambda^2-m^2}{q^2-m^2}\right)^2$$

is introduced to describe the structure effect of the $\mathrm{B}^{(*)}\mathrm{B}^{(*)}\pi$ and $\mathrm{B}^{(*)}\mathrm{B}^{(*)}\rho$ interaction vertices in Figs. 1 and 2. The parameter Λ introduced in the FF can be parameterized as $\Lambda=m+\alpha\Lambda_{\mathrm{QCD}}$ with $\Lambda_{\mathrm{QCD}}=220$ MeV, and m denotes the mass of the exchanged light meson. In the amplitudes a unique parameter α is introduced.

The total decay amplitudes are expressed as

$$\mathcal{A}_1 = \mathcal{M}_{\mathrm{a}}+\mathcal{M}_{\mathrm{b}}+\mathcal{M}_{\mathrm{c}}+\mathcal{M}_{\mathrm{a}}'+\mathcal{M}_{\mathrm{b}}'+\mathcal{M}_{\mathrm{c}}', \tag{7}$$

$$\mathcal{A}_2 = \mathcal{M}_{\mathrm{d}}+\mathcal{M}_{\mathrm{e}}+\mathcal{M}_{\mathrm{d}}'+\mathcal{M}_{\mathrm{e}}', \tag{8}$$

$$\mathcal{A}_3 = \mathcal{M}_1+\mathcal{M}_2+\mathcal{M}_1'+\mathcal{M}_2', \tag{9}$$

where $\mathcal{M}_i'$, $\{i=a-e,1-2\}$ are the corresponding am-

plitudes with η and/or ω exchange. The amplitudes $\mathcal{A}_1$ and $\mathcal{A}_2$ correspond to $\Upsilon(5S)\to\mathrm{B}^{*0}\mathrm{B}^-\pi^+$ with the intermediate $\mathrm{B}\bar{\mathrm{B}}^*+\mathrm{h.c.}$ and $\mathrm{B}^*\bar{\mathrm{B}}^*$, respectively, while $\mathcal{A}_3$ corresponds to $\Upsilon(5S)\to\mathrm{B}^{*0}\mathrm{B}^{*-}\pi^+$ with the intermediate $\mathrm{B}^*\bar{\mathrm{B}}^*$. The general differential decay width for $\Upsilon(5S)(p_0)\to\pi(p_3)\mathrm{B}^{(*)}(p_4)\mathrm{B}^*(p_5)$ is

$$\mathrm{d}\Gamma_i=\frac{1}{3}\frac{1}{(2\pi)^3}\frac{1}{32m_{\Upsilon(5S)}^3}\overline{|\mathcal{A}_i|^2}\mathrm{d}m_{\mathrm{B}^*\mathrm{B}^{(*)}}^2\mathrm{d}m_{\mathrm{B}^*\pi}^2,(i=1,2,3) \tag{10}$$

with $m_{\mathrm{B}^*\mathrm{B}^{(*)}}^2=(p_4+p_5)^2$ and $m_{\mathrm{B}^*\pi}^2=(p_3+p_5)^2$, where the overline indicates the sum over the polarization of $\Upsilon(5S)$ in the initial state and the polarizations of B^* or $\bar{\mathrm{B}}^*$ meson in the final state.

Here, we emphasize that some other decay mechanisms might also work in the hidden bottom pion decays of $\Upsilon(5S)$ and the interferences between different mecha-

nisms can affect the lineshapes of $B\bar{B}^*$ and $B^*\bar{B}^*$ invariant mass spectra. However, in the present work, we consider only the ISPE mechanism to check whether we can produce some enhancements near the thresholds of $B\bar{B}^*$ and $B^*\bar{B}^*$ with this mechanism, as we have shown for the hidden-bottom dipion decays of $\Upsilon(5S)$ and hidden-charm dipion decays of higher charmonia.

The lineshapes of the $B\bar{B}^*$ and $B^*\bar{B}^*$ invariant mass spectra distributions of $\Upsilon(5S)\to B^{*0}B^-\pi^+$ and $\Upsilon(5S)\to B^{*0}B^{*-}\pi^+$ decays are evaluated in an effective Lagrangian approach; however, the interference effects between $\mathcal{A}_1$ and $\mathcal{A}_2$ are not considered in this work. The coupling constants between $\Upsilon(5S)$ and the intermediate $B^*\bar{B}^{(*)}\pi$ are common factors appearing in front of the amplitudes $\mathcal{A}_i,\{i=1,2,3\}$; thus, they cannot affect the lineshapes. Furthermore, the shapes of the invariant mass distributions are weakly dependent on the parameter α introduced in the form factor. In the present work, we set $\alpha=1$. Calculating the distributions of Eq. (10), we can see whether there exist the enhancement structures close to the $B\bar{B}^*$ and $B^*\bar{B}^*$ thresholds originating from

the ISPE mechanism. In the present work, the interferences between ISPE mechanisms with different intermediate states are not included. Hence, direct comparison between present theoretical results and experimental measurements is not appropriate. Consequently, we only present the lineshapes of $B^*\bar{B}^{(*)}$ invariant mass spectra separately in Fig. (3). By comparing them with the experimental measurements, one can see that the positions of the peaks of our theoretical curves nicely match with those of the experimental enhancement structures.

3   The open-charm decays of higher charmonia with a single pion emission

Being inspired by the success of the former section, we would like to apply the ISPE mechanism to the open charm decays of higher charmonia with a single pion emission; for example, to the processes $\psi(4415)\to \pi^+D^{*0}D^{(*)-}$ and $\psi(4160)\to\pi^+D^{*0}D^-$.

What we need in this section is to replace $\Upsilon(5S)$, B, and B^* in Figs. 1 and 2 with $\psi(4415)/\psi(4160)$, D, and
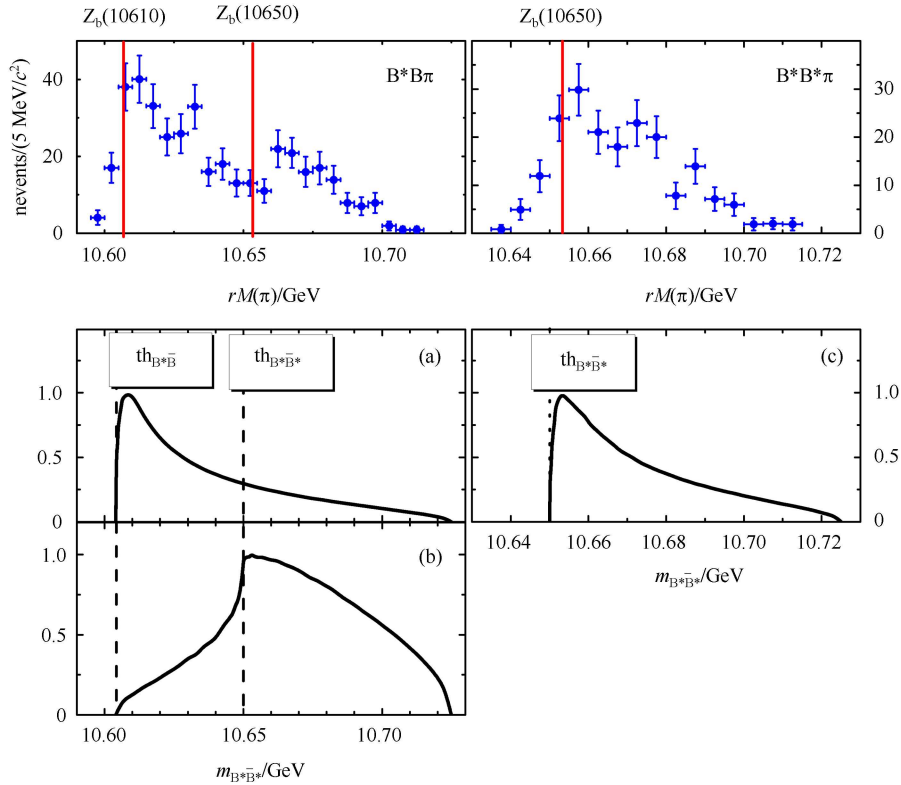

Fig. 3. (color online) The theoretical curves for distributions of $\mathrm{d}\Gamma(\Upsilon(5S)\to B^{*0}B^-\pi^+)/\mathrm{d}m_{B\bar{B}^*}$ (left) and $\mathrm{d}\Gamma(\Upsilon(5S)\to B^{*0}B^{*-}\pi^+)/\mathrm{d}m_{B^*\bar{B}^*}$ (right) (see diagrams (a)–(c)). Here, the maximum of the theoretical line shape is normalized to be 1 and the typical value of $\alpha=1$ is taken in our calculation. Diagrams (a) and (b) correspond to $\Upsilon(5S)\to B^{*0}B^-\pi^+$ via the intermediates $B\bar{B}^*$+h.c. and $B^*\bar{B}^*$, respectively, by the ISPE mechanism. Diagram (c) reflects the distribution $\mathrm{d}\Gamma(\Upsilon(5S)\to B^{*0}B^{*-}\pi^+)/\mathrm{d}m_{B^*\bar{B}^*}$ of $\Upsilon(5S)\to B^{*0}B^{*-}\pi^+$. To compare our theoretical results with the experimental data, we also show Belle's data (the blue dots with error) for the $\Upsilon(5S)\to B\bar{B}^*\pi$ (left) and $\Upsilon(5S)\to B^*\bar{B}^*\pi$ (right) [22]. The thresholds of $B\bar{B}^*$ and $B^*\bar{B}^*$ are marked by the dashed lines.
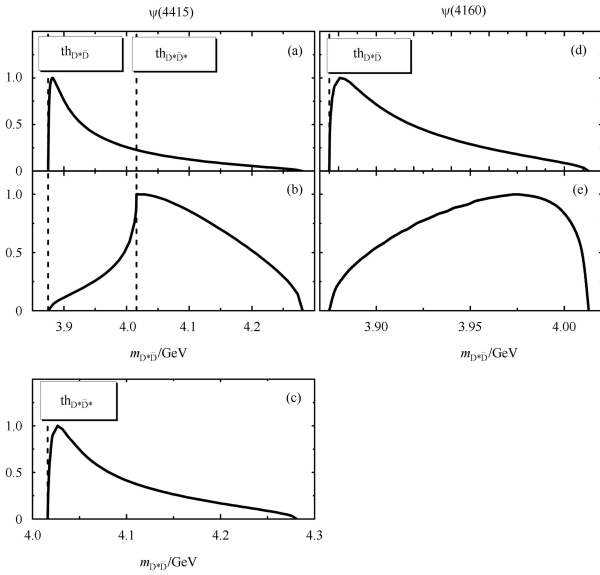
Fig. 4.   The theoretical curves for $D^*\bar{D}^{(*)}$ invariant mass spectrum in open charm pion decays of higher charmonia $\psi(4415)$ and $\psi(4160)$. The curves for $d\Gamma(\psi(4415) \to D^{*0}D^-\pi^+)/dm_{D^*\bar{D}}$ via $D^{*0}D^-$ and $D^{*0}D^{*-}$ in the ISPE framework correspond to diagrams (a) and (b), respectively. Diagram (c) indicates the ISPE mechanism prediction for $d\Gamma(\psi(4415) \to D^{*0}D^{*-}\pi^+)/dm_{D^*\bar{D}^*}$ via $D^{*0}D^{*-}$ intermediate. For $\psi(4160)$ only $D^*D\pi$ process is allowed, and diagrams (d) and (e) express $d\Gamma(\psi(4160) \to D^{*0}D^-\pi^+)/dm_{D^*\bar{D}}$ via $D^{*0}D^-$ and $D^{*0}D^{*-}$, respectively.

D^*, respectively. We also need to replace the corresponding fields in the effective Lagrangians in Eqs. (1–3). The parameters have, of course, new definitions. The resultant curves are shown in Fig. 4. Similarly to $\Upsilon(5S) \to$

$\pi B^*\bar{B}^{(*)}$, there are two significant enhancement structures near the thresholds of $D^*\bar{D}$ and $D^*\bar{D}^*$ in the invariant mass spectra $m_{D^*\bar{D}}$ and $m_{D^*\bar{D}^*}$ of $\psi(4415) \to \pi D^*\bar{D}^{(*)}$. For $\psi(4160) \to \pi D^*\bar{D}$, only one enhancement near the $D^*\bar{D}$ threshold is predicted and the threshold of $D^*\bar{D}^*$ is out of the range of the invariant mass spectra $m_{D^*\bar{D}}$ of this process.

4   Summary

Very recently, the Belle Collaboration has reported new results on $Z_b(10610)$ and $Z_b(10650)$ at the ICHEP2012 conference, which stated that these Z_b structures also exist in the $B\bar{B}^*$ and $B^*\bar{B}^*$ invariant mass spectra of $\Upsilon(5S) \to \pi B\bar{B}^*$, $\pi B^*\bar{B}^*$ decays [22]. This has motivated us to apply the ISPE mechanism, especially because these are the typical processes for this mechanism to be applied. Using the effective Lagrangian approach among hadrons, as well as chiral particles, we have computed the theoretical curves of the invariant mass spectra of $B^*\bar{B}^{(*)}$ for the above processes, which are shown in Figs. 3, and have achieved successful agreement with experimental enhancement structures of $Z_b(10610)$ and $Z_b(10650)$.

This success has further driven us to apply the ISPE mechanism to the open-charm decays of higher charmonia with a single pion emission, $\psi(4415) \to \pi^+D^{*0}D^-$ and $\psi(4160) \to \pi^+D^{*0}D^-$. Similar procedures to those in Section 2 have led us to depict the theoretical curves of the invariant mass spectra as shown in Fig. 4. It can be seen tha two clear peaks exist in the invariant mass spectra $m_{D^*\bar{D}}$ and $m_{D^*\bar{D}^*}$ of the decay $\psi(4415) \to \pi^+D^{*0}D^-$ and one peak for $m_{D^*\bar{D}}$ of $\psi(4160) \to \pi^+D^{*0}D^-$. These predictions can be easily tested by Bell, BaBar and the forthcoming BellII.

References

1   Bondar A et al. (Belle collaboration). Phys. Rev. Lett., 2012, **108**: 122001
2   Adachi I et al. (Belle collaboration). arXiv:1105.4583 [hep-ex]
3   LIU Y R, LIU X, DENG W Z et al. Eur. Phys. J. C, 2008, **56**: 63
4   LIU X, LUO Z G, LIU Y R et al. Eur. Phys. J. C, 2009,**61**: 411
5   Bondar A, Garmash A, Milstein A I et al. Phys. Rev. D, 2011, **84**: 054010
6   YANG Y, PING J, DENG C et al. J. Phys. G, 2012, **39**:105001
7   SUN Z F, HE J, LIU X, LUO Z G et al. Phys. Rev. D, 2011, **84**: 054002
8   Mehen T, Powell J W. Phys. Rev. D, 2011, **84**: 114013
9   ZHANG J R, ZHONG M, HUANG M Q. Phys. Lett. B, 2011, **704**: 312
10   KE H W, LI X Q, SHI Y L, WANG G L et al. JHEP, 2012, **1204**: 056
11   Voloshin M B. Phys. Rev. D,2011, **84**: 031502
12   LI X, Voloshin M B. Phys. Rev. D, 2012, **86**: 077502
13   Cleven M, GUO F K, Hanhart C et al. Eur. Phys. J. A, 2011, **47**: 120
14   DONG Y, Faessler A, Gutsche T et al. J. Phys. G, 2013, **40**: 015002
15   GUO T, CAO T, ZHOU M Z, CHEN H. arXiv:1106.2284 [hep-ph]
16   CUI C Y, LIU Y L, HUANG M Q. Phys. Rev. D, 2012, **85**: 074014
17   Ali A, Hambrock C, WANG W. Phys. Rev. D, 2012, **85**: 054011
18   Bugg D V. Europhys. Lett., 2011, **96**: 11002
19   CHEN D Y, LIU X, ZHU S L. Phys. Rev. D, 2011, **84**: 074016
20   CHEN K F et al. (Belle collaboration). Phys. Rev. Lett., 2008, **100**: 112001
21   CHEN D Y, LIU X. Phys. Rev. D, 2011, **84**: 094003
22   Bondar A (Belle collaboration). Talk Given in 36th International Conference on High Energy Physics (ICHEP2012)
23   CHEN D Y, LIU X. Phys. Rev. D,2011, **84**: 034032
24   Coffman D et al. (MARK-III collaboration). Phys. Rev. D, 1988, **38**: 2695; 1989, **40**: 3788
25   Jousset J et al. (DM2 collaboration). Phys. Rev. D,1990, **41**: 1389